

IMAGE INTERPRETATION FOR FIELDS  
PRODUCED BY HIGH FREQUENCY  
LINE CURRENTS OVER FINITE  
CONDUCTING MEDIA

By  
BRUCE EUGENE MATHEWS

A DISSERTATION PRESENTED TO THE GRADUATE COUNCIL OF  
THE UNIVERSITY OF FLORIDA  
IN PARTIAL FULFILLMENT OF THE REQUIREMENTS FOR THE  
DEGREE OF DOCTOR OF PHILOSOPHY

UNIVERSITY OF FLORIDA

April, 1964

## ACKNOWLEDGMENTS

The author wishes to acknowledge his gratitude to the members of his supervisory committee for their guidance. Particular thanks are given to the chairman, Dr. M. J. Larsen, for the constant encouragement and personal interest given during the author's entire graduate program.

Thanks are also given to Dr. T. S. George and Dr. C. B. Smith for their help in the mathematical aspects of the dissertation. Special acknowledgment is extended to Dr. M. H. Clarkson for his advice during the formulation of the problem.

## TABLE OF CONTENTS

	Page
ACKNOWLEDGMENTS . . . . .	ii
LIST OF ILLUSTRATIONS . . . . .	iv
ABSTRACT . . . . .	v
 SECTION	
I. INTRODUCTION . . . . .	1
General Problem . . . . .	1
Previous Studies . . . . .	6
II. FIELD EQUATIONS . . . . .	7
Bifilar Conductor Configuration . . . . .	7
General Field Relationships . . . . .	7
Equations Describing the Vector	
Magnetic Potential . . . . .	10
Source Potential . . . . .	11
Fourier Expansions of Potential	
Distributions . . . . .	12
III. DERIVATION OF MULTIPOLE IMAGES . . . . .	16
Asymptotic Approximation of Integral . . . . .	16
Potential Due to Single Line Source . . . . .	20
Line Multipole Interpretation . . . . .	24
Reflected Impedance Produced by	
Multipoles . . . . .	28
IV. SUMMARY AND CONCLUSIONS . . . . .	32
BIBLIOGRAPHY . . . . .	33
BIOGRAPHICAL SKETCH . . . . .	34

# LIST OF ILLUSTRATIONS

Figure		Page
1	Filamentary Conductor Parallel to Semi-Infinite Conducting Medium. . . . .	2
2	Image Conductor Produced by Perfect Reflection. . . . .	5
3	Cross Section of Bifilar Filamentary Line Currents . . . . .	8
4	Complex Coordinate Systems at Image Positions . . . . .	19
5	Single Filamentary Line Current . . . . .	22
6	Line Dipole Current at Image Position . . .	25
7	Line Quadrupole at Image Position . . . . .	27
8	Line Multipole with Six Currents. . . . .	29

Abstract of Dissertation Presented to the Graduate Council  
in Partial Fulfillment of the Requirements for the  
Degree of Doctor of Philosophy

IMAGE INTERPRETATION FOR FIELDS PRODUCED BY  
HIGH FREQUENCY LINE CURRENTS OVER FINITE  
CONDUCTING MEDIA

By

Bruce Eugene Mathews

April 18, 1964

Chairman: M. J. Larsen

Major Department: Electrical Engineering

The magnetic field distribution produced by a filamentary conductor in a nonconducting medium carrying sinusoidally time varying current parallel to a semi-infinite, finite conducting medium is considered. It is assumed that the wave length of the fields in the medium surrounding the filamentary conductor is large compared to the dimensions of the configuration so that retardation can be neglected. The study is devoted particularly to the high frequency case where the field penetration into the conducting medium is relatively small; that is, good reflection is obtained. If the medium has infinite conductivity, reflection is perfect and the resulting

field distribution can be calculated using a mirror image approach. The purpose of this study is to derive a modified image approach which can be used when the reflection is not perfect; that is, the medium has finite conductivity. The analysis is generalized with respect to the magnetic permeability of the medium.

An equation is derived for the vector magnetic potential produced in the region above the conducting medium. The resulting expression is interpreted as that potential produced by the source and its mirror image plus a potential described by an integral. An asymptotic series approximation to the integral reveals terms which can be interpreted as line multipoles of increasing order located at the mirror image position. These multipoles constitute a modification of the mirror image and can be used to describe nonperfect reflection.

## SECTION I

### INTRODUCTION

#### General Problem

A magnetic field problem which has many practical applications involves an infinitely long filamentary conductor in a nonconducting medium carrying sinusoidally time varying current parallel to the surface of a flat semi-infinite conducting medium. The configuration is illustrated in Figure 1 where the current is assumed to be  $Ie^{j\omega t}$ . This is the commonly employed exponential notation used to represent sinusoidal time variation at a frequency of  $\omega$  radians per second,  $j$  being  $\sqrt{-1}$ .

For this configuration to closely approximate a practical problem, it is not necessary that the medium extend to infinity, but only to distances large compared to the height of the conductor above the surface. The solution applies specifically to a conductor whose diameter is very small compared to the height. Or, if a larger conductor is involved, the result can be considered a superposition of many filamentary conductors. In summary, this specific problem is basic to a large class of magnetic field problems.

The author became interested in this problem while studying analytic methods of induction heating work-coil

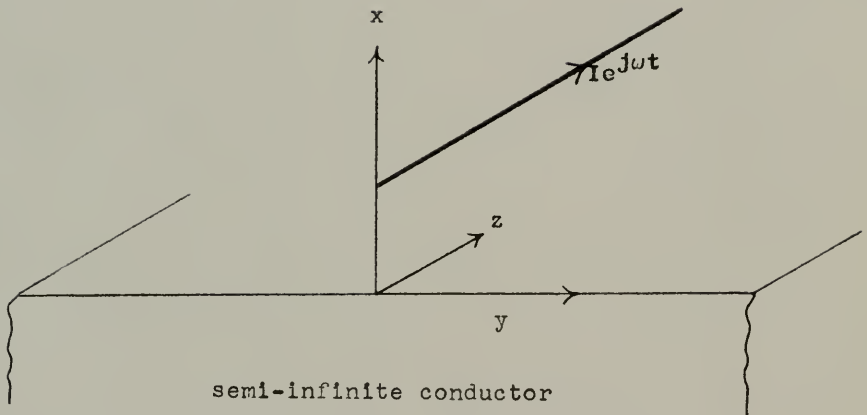


Figure 1. Filamentary Conductor Parallel to Semi-Infinite Conducting Medium.



design.<sup>1\*</sup> Induction heating involves placing a conductor configuration (called a work coil) carrying radio-frequency currents near the item to be heated. The time varying magnetic fields induce eddy currents in the item and produce heat. For the heating to be effective, the item must be a fairly good electrical conductor. Practical applications involve heating both ferromagnetic and non-ferromagnetic materials.

Designing a work coil for a specific test involves determining the conductor configuration which will give the desired heating pattern. The heating pattern is determined by the magnetic field distribution. It should be mentioned that the interest is in the induction field produced by the current since the dimensions of the coils are generally small compared with the free space wave length of the frequencies involved. Thus, retardation and the radiation field can be neglected in any analysis.

In Figure 1, the filamentary conductor represents part of the work coil and the semi-infinite conductor represents the item to be heated. The normal method of analyzing this type configuration is to first assume that the item is a perfect conductor; that is, its electrical conductivity is infinite. This is usually considered a good approximation since due to skin effect the magnetic field penetrates only a very small distance into the item.

---

\* Superscripts refer to numbered bibliography.

This, of course, depends on the magnitude of the frequency and the electrical conductivity. However, for most applications the penetration is quite small, since this is generally what is desired when heating by induction. The "perfect conductor" approximation merely assumes the penetration is zero which implies that the surface is a perfect reflector.

Having made this assumption, the field distribution above the surface can be easily calculated by replacing the effect of the reflector by a filamentary conductor located at the mirror image position of the work-coil conductor. This image conductor is assumed to carry a current equal in magnitude to the work-coil conductor but 180 degrees out of phase. This configuration, shown in Figure 2, produces the same boundary conditions as the perfect reflector. The procedure then is to base calculations of inductance and surface heating on the field distribution produced by the filamentary conductor and its image.

An interesting question arises as to the criterion which makes this approximation a valid one. One would assume that such a criterion would involve the relative magnitude of the penetration of the fields into the surface. Also, it would seem reasonable that some modification of the perfect image approach might be used to better the approximation for those cases which do not meet

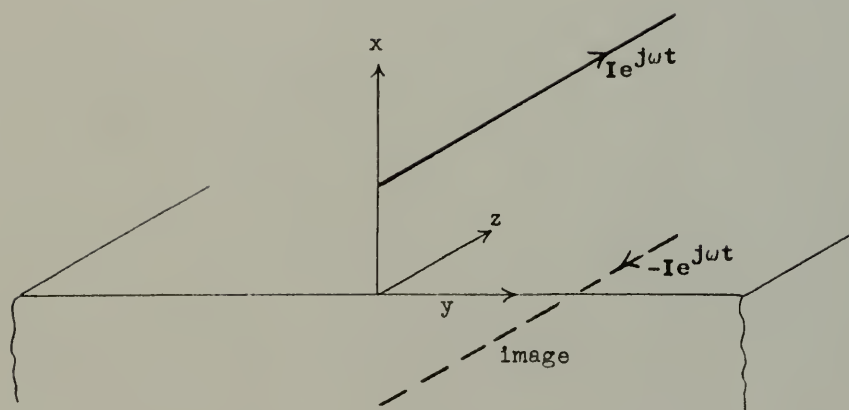


Figure 2. Image Conductor Produced by Perfect Reflection.

the criterion. A study of a modified image approach is the subject of this investigation.

### Previous Studies

A literature search revealed several studies in this general area. The reflection of nonperfect conductors has been studied by several investigators interested in the wave propagation from dipoles located above the finite conducting earth. Stratton<sup>2</sup> summarizes the early work of Sommerfeld, Van Der Pol, Weyl, and others on this problem. The analysis showed that part of the field above the earth could be interpreted as that produced by a perfect image. However, there remained an additional term involving an integral which was difficult to interpret. Attempts were made to approximate the integral but no clear interpretation in terms of images resulted.

Carson<sup>3</sup> analyzed a configuration exactly as that of Figure 1. However, he limited his study to nonferromagnetic conductors since his interest was in the effect of the earth on overhead transmission lines. He was able to obtain approximations to the field distributions in the form of an asymptotic series but made no attempt to interpret these results in terms of images.

## SECTION II

### FIELD EQUATIONS

#### Bifilar Conductor Configuration

It is convenient initially to set up the problem in terms of two long parallel filamentary lines with currents of equal magnitude but 180 degrees out of phase. This could represent a conductor and its return path joined a long distance away to form a closed circuit. A cross-section representation is shown in Figure 3. The lower half plane is occupied by a material with electrical conductivity  $\sigma_2$  and magnetic permeability  $\mu_2$ . The upper half plane is nonconducting with permeability  $\mu_1$ .

#### General Field Relationships

The analysis uses the concept of the vector magnetic potential,  $\bar{A}$ , where the general relationships between this vector and the electric and magnetic fields are

$$\nabla \times \bar{A} = \mu \bar{H}, \quad (1)$$

$$\nabla \cdot \bar{A} = -\mu\epsilon \frac{\partial V}{\partial t}, \quad (2)$$

$$\bar{E} = -\nabla V - \frac{\partial \bar{A}}{\partial t}, \quad (3)$$

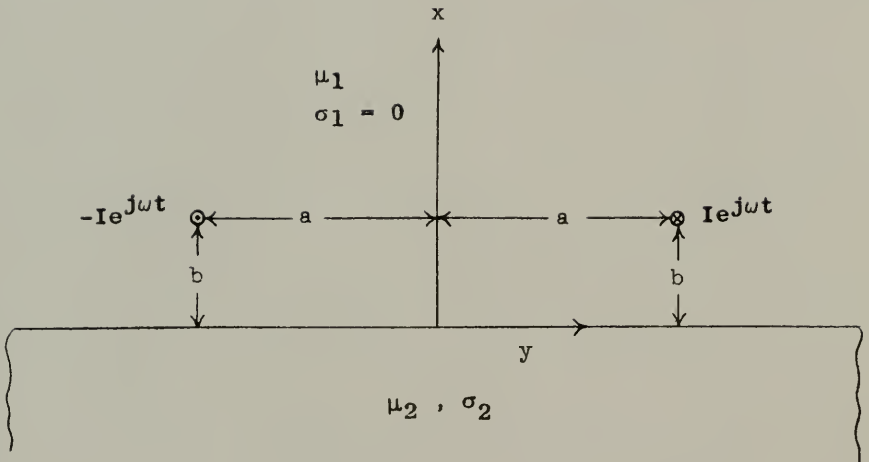


Figure 3. Cross Section of Bifilar Filamentary Line Currents.

where  $\vec{H}$  is the magnetic field intensity vector,  $\vec{E}$  is the electric field intensity vector,  $V$  is the scalar electric potential, and  $\epsilon$  is the dielectric constant of the medium.

First note that due to the configuration we have assumed, only a z-component of magnetic potential,  $A_z$ , will result since all of the current is in the z-direction. Also, recalling that we are dealing with frequencies whose free space wave length is very long compared with the dimensions of the configuration, we can assume that the current in the lines is uniform along the z-direction and in turn,  $A_z$  is not a function of  $z$ . This means that the divergence of  $\vec{A}$  is zero and from equation (2),  $\frac{\partial V}{\partial t}$  is zero. What we are really saying is that the conductors are short enough so that no appreciable standing wave is produced. Now, if we neglect any static potential,  $V$  is zero. Therefore, the equations (1), (2), and (3) reduce to

$$\nabla \times \vec{A} = \mu \vec{H}, \quad (4)$$

$$\nabla \cdot \vec{A} = 0, \quad (5)$$

$$\vec{E} = - \frac{\partial \vec{A}}{\partial t}. \quad (6)$$

Equations Describing the Vector Magnetic Potential

Taking the curl of both sides of (4) and using (5), we obtain

$$\nabla^2 \bar{A} = -\mu \nabla \times \bar{H}. \quad (7)$$

From Maxwell's equations for a general homogeneous medium,

$$\nabla \times \bar{H} = \sigma \bar{E} + \epsilon \frac{\partial \bar{E}}{\partial t}, \quad (8)$$

where the first term on the right represents the conduction current density and the second term the displacement current density.

Now consider the upper half plane of our configuration. Since it is nonconducting, the conduction current is zero except at the line currents. Also, if we neglect radiation we are in effect neglecting displacement current. Therefore, we are assuming that the curl of  $\bar{H}$  is zero except at the singularities produced at the line currents and equation (7) for the nonconducting region becomes

$$\nabla^2 \bar{A}_1 = 0, \quad (x > 0), \quad (9)$$

where the subscript "1" is used to denote the field in the upper half plane.

The medium in the lower half plane is assumed to be a fairly good conductor. This means that the conduction current is much greater than the displacement current at



the frequency being considered. Therefore, the second term in (8) can be neglected and (7) for this region becomes

$$\nabla^2 \bar{A}_2 = -\mu_2 \sigma_2 \bar{E}_2, \quad (x < 0), \quad (10)$$

where the subscript "2" refers to the lower half plane. Substituting (6) into (10) and assuming  $e^{j\omega t}$  time variation gives

$$\nabla^2 \bar{A}_2 = jk^2 \bar{A}_2, \quad (x < 0), \quad (11)$$

where

$$k^2 = \omega \mu_2 \sigma_2. \quad (12)$$

### Source Potential

Consider now the vector magnetic potential produced in the upper half plane by the two filamentary conductors, neglecting for a moment the effect of the lower half plane. Equation (9) shows that the field distribution is quasi-steady. That is, the spatial distribution is the same as that produced by a steady current. The resulting field is then merely the product of the time variation of the current and the steady spatial distribution. For line currents, the vector magnetic potential has the familiar logarithmic distribution. Therefore, the two lines alone produce a

z-component source potential,  $A_{sz}$ , given by

$$A_{sz} = \frac{\mu_1 I e^{j\omega t}}{4\pi} \ln \left[ \frac{(b-x)^2 + (y+a)^2}{(b-x)^2 + (y-a)^2} \right]. \quad (13)$$

### Fourier Expansions of Potential Distributions

The currents which are induced in the lower half plane will also contribute to the potential in the upper half plane. The resulting potential must also be a solution of (9). Again noting that there is only a z-component of potential and that this component is only a function of x and y, the Laplacian of  $\bar{A}$  in rectangular coordinates is

$$\nabla^2 \bar{A} = (\nabla^2 A_z) \bar{a}_z = \left[ \frac{\partial^2 A_{1z}}{\partial x^2} + \frac{\partial^2 A_{1z}}{\partial y^2} \right] \bar{a}_z, \quad (14)$$

where  $\bar{a}_z$  is the unit vector in the z-direction. Now (9) becomes

$$\frac{\partial^2 A_{1z}}{\partial x^2} + \frac{\partial^2 A_{1z}}{\partial y^2} = 0, \quad (x > 0). \quad (15)$$

A suitable solution of (15) can be written in terms of a Fourier expansion. For the symmetry in our case, a Fourier sine expansion is sufficient because the distribution is an odd function of y. Therefore, the potential distribution in the upper half plane can be written as

$$A_{1z} = e^{j\omega t} \int_0^\infty g_1(n) e^{-xn} \sin(yn) \, dn + A_{sz}, \quad (x > 0), \quad (16)$$

where the first term represents the contribution from the current in the lower half plane and the second term is due to the source currents and is given by Equation (13).

The potential distribution in the lower half plane must be a solution of (11), where the Laplacian of  $\bar{A}$  is defined by (14). Again using a Fourier sine expansion, we obtain as a generalized solution of (11)

$$A_{2z} = e^{j\omega t} \int_0^{\infty} g_2(n) e^{\sqrt{n^2 + jk^2} x} \sin(yn) \, dn, \quad (x < 0), \quad (17)$$

where the root with the positive real part is used.

The two functions  $g_1(n)$  and  $g_2(n)$  are determined by the boundary conditions at  $x = 0$ . These conditions require that the tangential electric and magnetic field intensity be continuous across the boundary. From (4) and (6), this requires that

$$\frac{1}{\mu_1} \frac{\partial A_{1z}}{\partial x} = \frac{1}{\mu_2} \frac{\partial A_{2z}}{\partial x}, \quad (x = 0), \quad (18)$$

$$A_{1z} = A_{2z}, \quad (x = 0). \quad (19)$$

Before the boundary conditions are applied, it is necessary to obtain an integral representation of equation (13). From Bateman,<sup>4</sup>

$$\int_0^{\infty} e^{-pt} \sin(\alpha t) \sin(\beta t) \frac{dt}{t} = \frac{1}{4} \ln \left[ \frac{p^2 + (\alpha + \beta)^2}{p^2 + (\alpha - \beta)^2} \right],$$

$$\operatorname{Re} p > |\operatorname{Im} (\pm \alpha \pm \beta)|, \quad (20)$$

where Re and Im indicate "the real part of" and the "imaginary part of" respectively. Therefore, (13) can be written

$$A_{sz} = \frac{\mu_1 I e^{j\omega t}}{\pi} \int_0^{\infty} e^{-(b-x)n} \sin(yn) \sin(an) \frac{dn}{n},$$

(0 < x < b). (21)

Substituting (21) into (16) and using (17) and (18), we obtain

$$\frac{1}{\mu_1} \left[ -ng_1(n) + \frac{\mu_1 I}{\pi} e^{-bn} \sin(an) \right] = \frac{1}{\mu_2} \sqrt{n^2 + jk^2} g_2(n). \quad (22)$$

Applying the boundary condition (19) gives

$$g_1(n) + \frac{\mu_1 I}{n\pi} e^{-bn} \sin(an) = g_2(n). \quad (23)$$

Combining (22) and (23) and letting  $\mu_1/\mu_2 = \mu'$ ,

$$g_1(n) = \frac{\mu_1 I}{n\pi} e^{-bn} \sin(an) \left[ \frac{2n}{n + \mu' \sqrt{n^2 + jk^2}} - 1 \right], \quad (24)$$

and (16) becomes

$$A_{1z} = \frac{\mu_1 I e^{j\omega t}}{\pi} \int_0^{\infty} \left[ \frac{2n}{n + \mu' \sqrt{n^2 + jk^2}} - 1 \right] e^{-(b+x)n} \sin(yn) \cdot \sin(an) \frac{dn}{n} + A_{sz}. \quad (25)$$

Now note that by (20), the second term in the integral of (25) is

$$\begin{aligned} & \frac{-\mu_1 I e^{j\omega t}}{\pi} \int_0^{\infty} e^{-(b+x)n} \sin(yn) \sin(an) \frac{dn}{n} \\ &= \frac{-\mu_1 I e^{j\omega t}}{4\pi} \ln \left[ \frac{(b+x)^2 + (y+a)^2}{(b+x)^2 + (y-a)^2} \right]. \end{aligned} \quad (26)$$

Comparing with (13), equation (26) describes the field produced by two filamentary currents located at  $x = -b$  and  $y = +a$ ; that is, the mirror image positions of the two source currents. Also, the negative sign indicates that the currents in the images are 180 degrees out of phase with the currents in the sources. These are exactly the mirror images produced with perfect reflection. Denoting this image potential described by (26) as  $A_{1z}$ , we can rewrite (25) as

$$\begin{aligned} A_{1z} = & \frac{2\mu_1 I e^{j\omega t}}{\pi} \int_0^{\infty} \frac{n}{n + \mu' \sqrt{n^2 + jk^2}} e^{-(b+x)n} \sin(yn) \\ & \cdot \sin(an) \frac{dn}{n} + A_{sz} + A_{1z}, \end{aligned} \quad (x > 0). \quad (27)$$

The first term in (27) describes that potential which is not accounted for by the mirror images. The purpose of the next discussion is to show that this remaining potential can be interpreted as being produced by line multipoles located at the image positions.

### SECTION III

#### DERIVATION OF MULTIPOLE IMAGES

##### Asymptotic Approximation of Integral

For purposes of discussion, denote the first term in (27) as  $A_{rz}$ .

$$A_{rz} = \frac{2\mu_1 I_0 e^{j\omega t}}{\pi} \int_0^{\infty} \frac{n}{n + \mu' \sqrt{n^2 + jk^2}} e^{-(b+x)n} \sin(yn) \cdot \sin(an) \frac{dn}{n} \quad (28)$$

The main task now is to find an interpretation of this integral which will give insight to its significance and also make more practical the calculation of the field distributions which it describes.

After much investigation involving various methods, the most useful approach appears to be one involving an asymptotic approximation to the integral. To form this approximation, part of the integral is expanded in a Taylor's series about  $n = 0$ ; namely,

$$\begin{aligned}
f(n) &= \frac{n}{n + \mu' \sqrt{n^2 + jk^2}} \\
&= f(0) + f'(0)n + \frac{f''(0)n^2}{2!} + \frac{f'''(0)n^3}{3!} + \dots \\
&= e^{-j\pi/4} \frac{n}{\mu'k} - e^{-j\pi/2} \left[ \frac{n}{\mu'k} \right]^2 \\
&\quad + e^{-j3\pi/4} \left[ 1 - \frac{\mu'^2}{2} \right] \left[ \frac{n}{\mu'k} \right]^3 - \dots \quad (29)
\end{aligned}$$

Note that  $f(n)$  has branch points at  $\pm ke^{j3\pi/4}$  and poles at  $\pm k\mu'e^{j\pi/4}/(1 - \mu'^2)^{1/2}$ , which means that (29) has a finite radius of convergence for finite  $k$ . The integral, on the other hand, extends to infinity. The result of replacing  $f(n)$  by the series in (29) and integrating (28) term by term is an asymptotic series which will give a good approximation for large values of  $k$ . Since this is the high frequency case, the series gives useful results for the problem being investigated. A good discussion of asymptotic approximations is presented by Jeffreys.<sup>5</sup>

The terms resulting from the expansion of  $f(n)$  and the subsequent integration can be identified as repeated derivatives of the mirror image potential,  $A_{1z}$ , as defined by equation (26), by noting that

$$\begin{aligned}
\frac{\partial^{(p)}(A_{1z})}{\partial x^{(p)}} &= (-1)^{p+1} \frac{\mu_1 I e^{j\omega t}}{\pi} \int_0^\infty n^p e^{-(b+x)n} \sin(yn) \\
&\quad \cdot \sin(an) \frac{dn}{n}, \quad (p = 0, 1, 2, 3 \dots) \quad (30)
\end{aligned}$$

Therefore, equation (28) can be expanded as

$$A_{rz} = 2 \left[ \frac{e^{-j\pi/4}}{\mu'k} \frac{\partial(A_{1z})}{\partial x} + \frac{e^{-j\pi/2}}{(\mu'k)^2} \frac{\partial^2(A_{1z})}{\partial x^2} + \left(1 - \frac{\mu'^2}{2}\right) \frac{e^{-j3\pi/4}}{(\mu'k)^3} \frac{\partial^3(A_{1z})}{\partial x^3} + \dots \right]. \quad (31)$$

To develop further the significance of  $A_{rz}$ , it is necessary to derive meaningful expressions for the repeated derivatives of  $A_{1z}$ . This operation is simplified by using the theory of complex variables. With each image position, we identify a complex variable coordinate system as shown in Figure 4, and define

$$\begin{aligned} u_1 &= r_1 e^{j\theta_1} = x_1 + jy_1, \\ u_2 &= r_2 e^{j\theta_2} = x_2 + jy_2. \end{aligned} \quad (32)$$

Equation (26) expressing the mirror image potential can now be written

$$A_{1z} = \frac{\mu_1 I_0 e^{j\omega t}}{2\pi} (\ln r_1 - \ln r_2). \quad (33)$$

Noting that

$$\begin{aligned} \ln u_1 &= \ln r_1 + j\theta_1, \\ \ln u_2 &= \ln r_2 + j\theta_2, \end{aligned} \quad (34)$$

and observing that the two functions in (34) are analytic



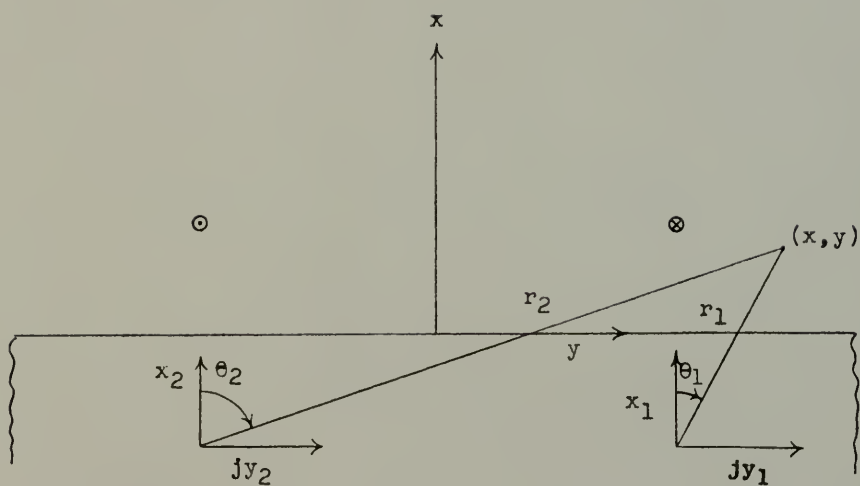


Figure 4. Complex Coordinate Systems at Image Positions.

(except at the origin), we can write

$$\frac{\partial^{(p)}(\ln r_1)}{\partial x_1^{(p)}} = \operatorname{Re} \left[ \frac{d^{(p)}(\ln u_1)}{du_1^{(p)}} \right] = (-1)^{p+1} (p-1)! \frac{\cos p\theta_1}{r_1^p},$$

$$\frac{\partial^{(p)}(\ln r_2)}{\partial x_2^{(p)}} = \operatorname{Re} \left[ \frac{d^{(p)}(\ln u_2)}{du_2^{(p)}} \right] = (-1)^{p+1} (p-1)! \frac{\cos p\theta_2}{r_2^p},$$

$$(p = 1, 2, 3, \dots), \quad (35)$$

where Re indicates that only the real part of the expression is used. Since the partial derivatives with respect to  $x_1$  and  $x_2$  equal that with respect to  $x$ , equation (31) can be written

$$\begin{aligned} A_{rz} = & \frac{\mu_1 I e^{j\omega t}}{\pi} \left[ \frac{e^{-j\pi/4}}{\mu'k} \left( \frac{\cos \theta_1}{r_1} - \frac{\cos \theta_2}{r_2} \right) \right. \\ & - \frac{e^{-j\pi/2}}{(\mu'k)^2} \left( \frac{\cos 2\theta_1}{r_1^2} - \frac{\cos 2\theta_2}{r_2^2} \right) \\ & \left. + (2-\mu'^2) \frac{e^{-j3\pi/4}}{(\mu'k)^3} \left( \frac{\cos 3\theta_1}{r_1^3} - \frac{\cos 3\theta_2}{r_2^3} \right) - \dots \right]. \quad (36) \end{aligned}$$

### Potential Due to Single Line Source

Up to this point, we have been dealing with two line current sources. This was convenient since it enabled the use of the integral representation of equation (21). We

can now investigate a single source by letting the distance between the two conductors become large compared to the distance each is above the surface. This in effect isolates the two conductors from each other. Assuming  $a \gg b$  and limiting our attention to the fields in the vicinity of the source at  $y = a$ ,  $r_2$  will become much larger than  $r_1$  and equation (36) can be written

$$A_{rz} = \frac{\mu_1 I e^{j\omega t}}{\pi} \left[ \frac{e^{-j\pi/4}}{\mu' k r_1} \cos \theta_1 - \frac{e^{-j\pi/2}}{(\mu' k r_1)^2} \cos 2\theta_1 + (2 - \mu'^2) \frac{e^{-j3\pi/4}}{(\mu' k r_1)^3} \cos 3\theta_1 - \dots \right] \quad (37)$$

This, then, is the potential, in addition to the source and its mirror image, which is produced in the upper half plane by a single filamentary current. The total potential in the upper half plane produced by a single filament located at  $x = b$ ,  $y = 0$  is

$$A_{1z} = \frac{\mu_1 I e^{j\omega t}}{2\pi} \left[ \ln \frac{r_1}{r} + \frac{2e^{-j\pi/4}}{(\mu' k r_1)} \cos \theta_1 - \frac{2e^{-j\pi/2}}{(\mu' k r_1)^2} \cos 2\theta_1 + 2(2 - \mu'^2) \frac{e^{-j\pi/4}}{(\mu' k r_1)^3} \cos 3\theta_1 - \dots \right], \quad (x > 0), \quad (38)$$

where the first term represents the source and its mirror image and  $r$ ,  $r_1$ , and  $\theta_1$ , are defined in Figure 5.

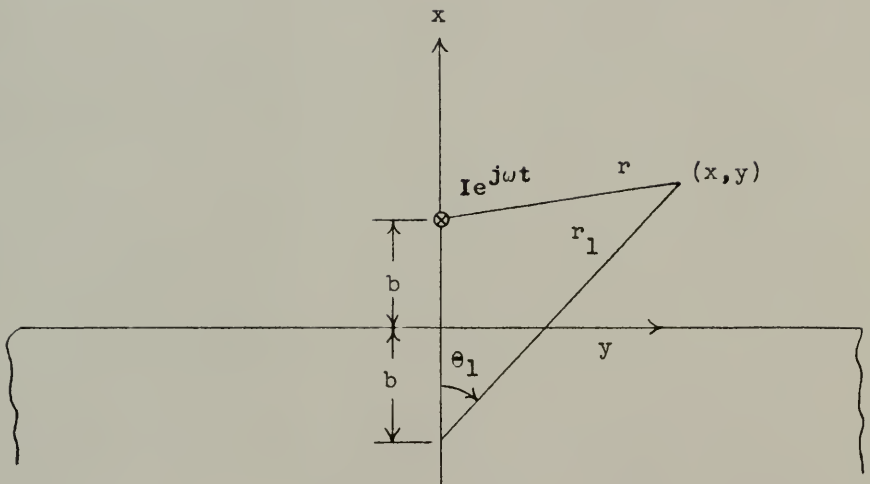


Figure 5. Single Filamentary Line Current.

Equation (38) is the result desired since it produces a useful asymptotic approximation for high frequencies. Note that convergence is largely dependent on the product  $(\mu'kr_1)$ . Only a few terms are necessary to give a good approximation if this product is much greater than unity. As the product approaches infinity, the fields approach a distribution produced by perfect reflection. A useful physical interpretation of this convergence requirement can be obtained by noting that

$$k = \sqrt{\omega\mu_2\sigma_2} = \sqrt{2}/\delta_2, \quad (39)$$

where  $\delta_2$  is the "depth of penetration," a factor commonly used to give a measure of the high frequency skin effect. Rapid convergence, then, requires

$$\mu'kr_1 \gg 1 \quad (40)$$

or,

$$r_1 \gg \frac{1}{\sqrt{2}} \frac{\mu_2}{\mu_1} \delta_2. \quad (41)$$

Equation (41) is interesting since it shows that perfect reflection is not justified entirely by a penetration small compared to the other dimensions. The ratio of magnetic permeabilities also enter into the criterion. However, this is entirely reasonable when one considers how the field distribution is dependent on this ratio even with steady currents.

### Line Multipole Interpretation

To give a physical interpretation of the terms in equation (38), assume the conducting medium in the lower half plane is removed and a pair of long filamentary conductors spaced a distance  $2d$  apart with currents 180 degrees out of phase are placed near the image position as shown in Figure 6. Again, using the complex variable notation of equation (32), the vector magnetic potential produced by the pair is

$$\begin{aligned} A_z &= \frac{\mu_1 I_1 e^{j\omega t}}{2\pi} \operatorname{Re} \left[ \ln \left( \frac{u_1 + d}{u_1 - d} \right) \right] \\ &= \frac{\mu_1 I_1 e^{j\omega t}}{2\pi} \operatorname{Re} \left[ \ln \left( 1 + \frac{2d}{u_1 + d} \right) \right]. \end{aligned} \quad (42)$$

Now, if we let  $d \ll r_1$ ,

$$\begin{aligned} A_z &\approx \frac{\mu_1 I_1 e^{j\omega t}}{2\pi} \operatorname{Re} \left[ \frac{2d}{u_1} \right] \\ &\approx \frac{\mu_1 I_1 e^{j\omega t}}{2\pi} \left( \frac{2d \cos \theta_1}{r_1} \right). \end{aligned} \quad (43)$$

With the restriction that  $d \ll r_1$ , the configuration of Figure 6 forms a line dipole and equation (43) describes the resulting field. Therefore, the second term in equation (38) represents such a line dipole with a current

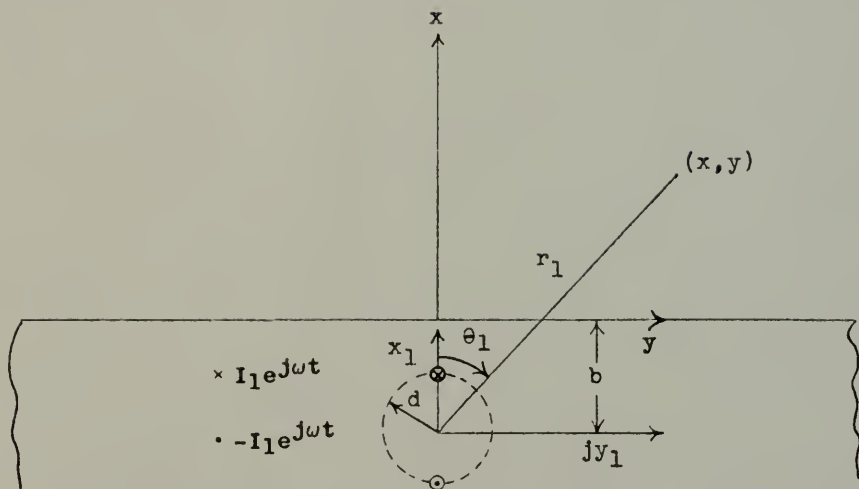


Figure 6. Line Dipole Current at Image Position.

$$I_1 = \frac{I e^{-j\pi/4}}{d \mu'_k} . \quad (44)$$

Note that the dipole current is not in phase with the source current.

To interpret the third term in (38), consider a line quadrupole as shown in Figure 7. Using the same approach as with the dipole, the resulting potential is

$$\begin{aligned} A_z &= \frac{\mu_1 I_2 e^{j\omega t}}{2\pi} \operatorname{Re} \left[ \ln \left( \frac{(u_1+d)(u_1-d)}{(u_1+jd)(u_1-jd)} \right) \right] \\ &= \frac{\mu_1 I_2 e^{j\omega t}}{2\pi} \operatorname{Re} \left[ \ln \left( 1 - \frac{2d^2}{u_1^2 + d^2} \right) \right] . \end{aligned} \quad (45)$$

Again letting  $d \ll r_1$ ,

$$A_z \approx \frac{\mu_1 I_2 e^{j\omega t}}{2\pi} \left( - \frac{2d^2 \cos 2\theta_1}{r_1^2} \right) . \quad (46)$$

The third term in (38) then represents this type quadrupole with current

$$I_2 = \frac{I e^{-j\pi/2}}{(d \mu'_k)^2} . \quad (47)$$

By a similar approach, the third term in (38) represents a line multipole involving six currents as



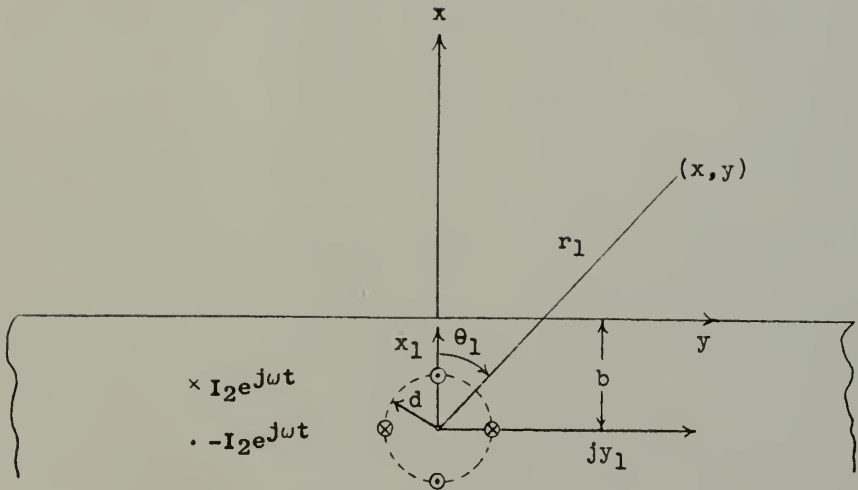


Figure 7. Line Quadrupole at Image Position.

shown in Figure 8 with current

$$I_3 = (2 - \mu'^2) \frac{I e^{-j3\pi/4}}{(d\mu'_k)^3} . \quad (48)$$

The multipole interpretation is more meaningful if we let

$$\begin{aligned} d &= 1/(\mu'_k) \\ &= \frac{1}{\sqrt{2}} \frac{\mu_2}{\mu_1} \delta_2 . \end{aligned} \quad (49)$$

Using this spacing gives multipole currents of the same order of magnitude as the source current. Note that (49) still satisfies the requirement  $d \ll r_1$  if the high frequency approximation is valid as stated by equation (41).

#### Reflected Impedance Produced by Multipoles

Another view of the significance of the asymptotic expansion can be obtained by viewing the effect of each multipole in terms of its contribution to the electrical impedance of the line source. From equations (6) and (37), the electric field produced by the multipoles,  $E_{rz}(r_1, \theta_1)$ , at the source is

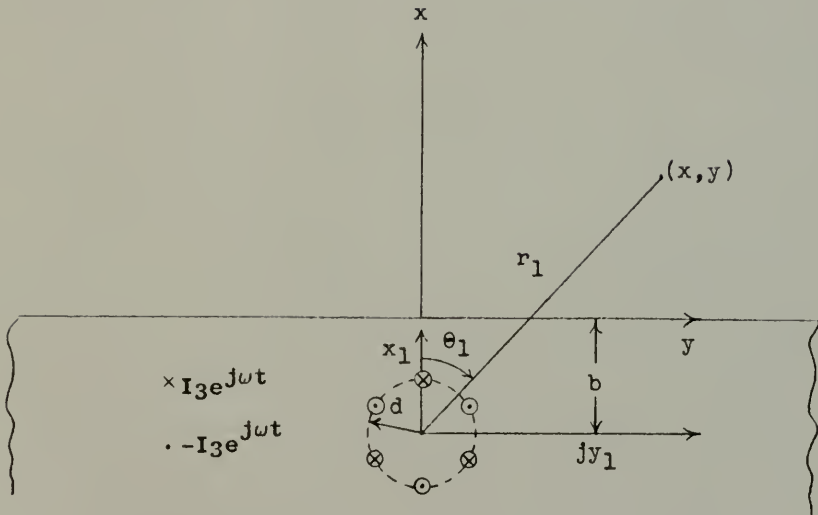


Figure 8. Line Multipole with Six Currents.

$$\begin{aligned}
 E_{rz}(2b,0) &= - \frac{\partial A_{rz}(2b,0)}{\partial t} \\
 &= \frac{-j\omega \mu_1 I_e j\omega t}{\pi} \left[ \frac{e^{-j\pi/4}}{\mu' k 2b} - \frac{e^{-j\pi/2}}{(\mu' k 2b)^2} \right. \\
 &\quad \left. + (2-\mu'^2) \frac{e^{-j3\pi/4}}{(\mu' k 2b)^3} - \dots \right] . \quad (50)
 \end{aligned}$$

The impedance per unit length,  $Z_r$ , due to this electric field can be defined in terms of the voltage drop produced, as

$$Z_r = - \frac{E_{rz}(2b,0)}{I_e j\omega t} = R_r + j\omega L_r . \quad (51)$$

With this approach, we obtain

$$R_r = \frac{\omega \mu_1}{\pi} \left[ \frac{1}{\mu' k 2b \sqrt{2}} - \frac{1}{(\mu' k 2b)^2} + \frac{(2-\mu'^2)}{\sqrt{2}(\mu' k 2b)^3} - \dots \right] , \quad (52)$$

$$j\omega L_r = \frac{\omega \mu_1}{\pi} \left[ \frac{1}{\mu' k 2b \sqrt{2}} - \frac{(2-\mu'^2)}{\sqrt{2}(\mu' k 2b)^3} + \dots \right] . \quad (53)$$

It should be emphasized that the electric field produced by the source itself and its mirror image also contribute to the total impedance. This is the impedance which would result if perfect reflection were obtained. Using a coupled circuit analogy, the impedance given by equation (51) can be considered an additional "reflected

impedance" due to the currents which actually flow in the conducting medium. The resistance term,  $R_p$ , is due to the power loss and the inductance,  $L_p$ , is due to the energy stored in the magnetic field inside the conducting medium.

The first term in equations (52) and (53) is supplied by the dipole image. It is interesting to note that this is exactly the approximation obtained if one first calculates the field distribution at the surface of the conducting medium based on perfect reflection, and then uses this surface field distribution to calculate the losses and stored energy in the medium. This approach is often used in problems of this type.

The quadrupole supplies the second term in (52) but does not contribute to (53). The multipole involving six sources produces an impedance defined by the last term in (52) and (53).

## SECTION IV

### SUMMARY AND CONCLUSIONS

Practical approximations to the fields produced by high frequency currents and good conducting media can often be obtained by assuming perfect reflection. This analysis has attempted to shed some light on the basis for this assumption by considering the specific case of filamentary line currents parallel to a flat semi-infinite, finite conducting medium. If perfect reflection were obtained, the effect of the medium could be replaced by mirror images of the line currents. The analysis shows that nonperfect reflection can be approximated by multipole images located at the mirror image positions. These multipoles produce an asymptotic approximation which converges fairly rapidly when good reflection is obtained.

It would be interesting to extend this analysis to finite conductors which are not parallel to the surface, other boundary shapes, and cases involving retardation effects. One might expect to obtain similar modified image approximations for these cases.

## BIBLIOGRAPHY

1. B. E. Mathews, "Flat Work-Coil Design,"  
Transactions of the AIEE, Vol. 7, Part II,  
pp. 249-256; November, 1957.
2. J. A. Stratton, "Electromagnetic Theory,"  
McGraw-Hill Book Co., Inc., New York and  
London, pp. 573-587; 1941.
3. J. R. Carson, "Wave Propagation in Overhead  
Wires with Ground Return," Bell System Journal,  
Vol. 5, pp. 539-554; October, 1926.
4. Bateman Manuscript Project, "Tables of Integral  
Transforms," Vol. 1, McGraw-Hill Book Co., Inc.,  
New York, p. 159; 1954.
5. H. Jeffreys, "Asymptotic Approximations,"  
Oxford University Press, London; 1962.

## BIOGRAPHICAL SKETCH

Bruce Eugene Mathews was born June 1, 1929, at Peru, Illinois. After he was graduated from Duncan U. Fletcher High School at Jacksonville Beach, Florida, he attended the University of Florida where he received the degrees Bachelor of Electrical Engineering and Master of Science in Engineering in 1952 and 1953, respectively. He then served in the United States Air Force from 1953 until 1955. After working for one year with North American Aviation Corporation in Los Angeles, California, he returned to the University of Florida in 1956. Since then until the present time, he has pursued his work toward the degree of Doctor of Philosophy while teaching and conducting research in the Department of Electrical Engineering as a Research Associate.

Bruce Eugene Mathews is married to the former Donna Lee Breazeale and is the father of three children. He is a member of the Institute of Electrical and Electronics Engineers, Sigma Tau, Phi Kappa Phi, and Tau Beta Pi.



April 18, 1964

Dean, Graduate School

C. B. Smith

